

Application Axicons in a Large-Aperture Focusing System

S. N. Khonina^{a, b} and S. G. Volotovskiy^a

^a*Image Processing Systems Institute, Russian Academy of Sciences, Samara*

^b*Samara State Aerospace University*

e-mail: khonina@smr.ru

Received April 22, 2014; in final form, September 9, 2014

Abstract—We consider the application of axicons in large-aperture focusing systems with different polarization. The aim is to increase the longitudinal extent of the focal spot and decrease its transversal size. Unlike conventional circular diaphragms, supplementing a high-aperture lens with an axicon is more efficient from the energetic point of view. The gain is proportional to the area of the masked part of the lens. Using an axicon we reduce the size of the central light spot from 0.51λ to 0.3λ for radial polarization. When we deal with linear polarization, which is the case for most laser beams, it is possible to produce a light spot narrowed in one direction to 0.32λ . For circular and azimuthal polarization it is efficient to use spiral axicons for producing compact distributions. When a large-aperture lens is supplemented even with a “weak” converging axicon, the focal area gets the conic form whose vertex has a smaller transverse dimension than the focal spot of a single lens. By choosing the axicon parameters we can vary the extent and “sharpness” of the cone. Moreover, by adding vortex phase we can control the contribution of different components of the electromagnetic field in the core and vertex of the cone. It can be useful in interaction of the electromagnetic field with the materials that have selective sensitivity to either longitudinal or transverse components of the field.

Keywords: diffractive linear axicon, lensacon, sharp focusing, central light spot size, depth of focus

DOI: 10.3103/S1060992X14040043

INTRODUCTION

Relying on the paraxial scalar model, paper [1] showed that a lensacon [2] consisted of two small-aperture elements (lens and axicon) can produce a central light spot whose size corresponds to a non-linear increase of the numerical aperture of the tandem. A tandem like that having at least one large-aperture element requires more exact theory. In our paper we consider linear and spiral axicons as supplements to a large-aperture lens in terms of sharp-focusing system in the Debye approximation.

The aim of many researches in large-aperture focusing system is to decrease the transverse size of the focal spot or/and increase the extent of the focal depth. The best results in this field have been achieved for radially polarized incident light [3–8]. As it is radial polarization that provides the best transfer of energy into the z -component of the electric field in the focus.

However, even in this case the theoretical limit related to the size of the Bessel zero-order beam (full width at half maximum FWHM = 0.36λ) remains unrealizable [9]. The thing is that in spite of the strong longitudinal component, the transverse components also make a sufficient contribution in the focal intensity, thus broadening the total size of the central spot. Additional efforts are needed to minimize the contribution of transverse components in the focal area. Particularly, a narrow ring diaphragm is offered in [3, 5] to allow only rays with the largest angle to the optical axis to reach the focus. Though simple to be realized, the method leads to a considerable loss of efficiency.

The parabolic mirror [10, 11], diffractive lens [10], micro-axicon [8] are the elements that can be used to increase the longitudinal component for full-aperture systems. All these kinds of optical elements should have large numerical aperture. Therefore, in the case of diffractive elements, the micro relief will have sub-wavelength zones which are difficult to fabricate.

There are also research works that use zone plates [9, 12, 13] and special algorithms to compute the zone radii for particular parameters of used focusing system. To avoid the loss of efficiency, the number of zones should not exceed three [13].

Here we offer phase axicons as full-aperture optical elements that can remove transverse components from the focal plane in the sharp focusing of a radially polarized beam. When a large-aperture lens is supplemented even with a “weak” converging axicon, the focal area looks like a cone whose vertex has a smaller

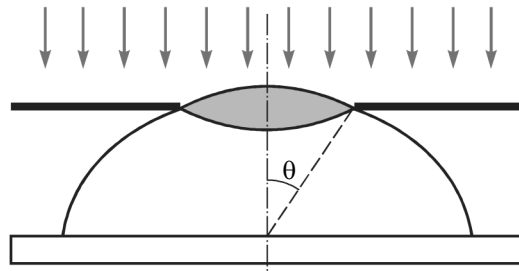


Fig. 1. The apertural angle of an aplanatic lens.

transverse dimension than the focal spot of a single lens. It is because the axicon increases the numerical aperture of central rays of the lens and redirect them from the focal plane closer to the lens plane. It is possible to vary the extent and “sharpness” of the cone by changing the parameters of the axicon.

The strengthening of the longitudinal components of the vector field is useful for not only decreasing the focal spot, but also in optical tweezers and 3D manipulation of molecules [14–17], electron acceleration [18, 19] and other applications [12]. It is interesting that in [20] excitation of individual fluorescent molecules was used to separate the components of a radially polarized beam.

Not only the longitudinal component of the electric field, but also the transverse components are useful. Particularly, in hollow metallic waveguides radially polarized beams lose more energy on the waveguide walls than azimuthally polarized ones [21]. Additionally, different components of the vector electromagnetic field can be used for three-dimensional excitation of fluorescent molecules [22].

We also show that with linearly polarized incident beams (the case of most laser beams) a large-aperture lensacon can be used to produce the focal spot whose area at half maximum (HMA) is 0.139λ instead of 0.237λ for a single lens. However, because of side lobes (consisting mostly of longitudinal components) the total electric field (the sum of intensities of all components) in the focus looks narrowed in one direction. It is possible to reduce the light spot dimension in this direction to 0.32λ .

It is shown that spiral axicons [23, 24] can be used effectively in generation of compact distributions for circular and azimuthal polarization. In this case it is possible to compensate the polarization singularity [25] existing in circular polarization and generate axially symmetric small focal spot. With azimuthal polarization we get a similar result except that the focal spot is more compact in this case due to the missing longitudinal component.

The possibility to achieve the sub-wavelength localization of different components of the vector electric field with the help of a vortex phase is considered in paper [26]. It is shown in the research that the vortex phase in the axicon allows us to regulate the contribution of the field components in the core and the vertex of the focal cone, which can be useful in controlled interaction of the electromagnetic field with materials exhibiting different sensitivity to the longitudinal and transverse components of the field [27].

1. THE LENSACON: MEDIUM-SIZED APERTURE, PARAXIAL SCALAR MODEL

When the plane wave bounded by a round diaphragm of radius R falls on a spherical lens of focal length f , the lens generates an intensity distribution in the focal plane which is proportional [28] to $J_1(k\rho Rf^{-1})\rho^{-1}$, $k = 2\pi/\lambda$. The central spot of the distribution has the radius determined by the first zero of Bessel function of the first kind $J_1(\gamma_{11}) = 0$, $\gamma_{11} = 3.83$.

So the least radius of the focal spot that a lens with a round diaphragm can produce is defined by the formula:

$$\rho_{\text{lens}} = \frac{3.83\lambda f}{2\pi R} = 1.22 \frac{\lambda f}{2R}. \quad (1)$$

Let us turn to the expression for the numerical aperture of aplanatic lenses in a medium with refractive index n :

$$NA_{\text{lens}} = n \sin \theta \approx n \frac{R}{f}, \quad (2)$$

where θ is so-called aperture angle of the lens (Fig. 1).

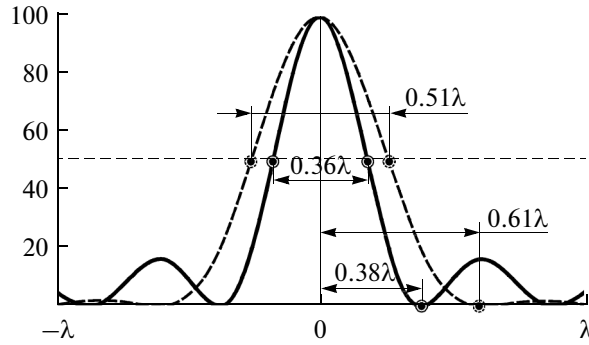


Fig. 2. The focal spot size for a lens (dashed line) and axicon (solid line).

Then it is possible to estimate the smallest radius of the focal spot in the free space as:

$$\rho_{\text{lens}} = \frac{0.61}{NA} \lambda \geq 0.61 \lambda. \quad (3)$$

The size of the focal spot can also be determined by the full width at the half maximum (FWHM) of the focal-plane intensity profile (Fig. 2). In the case of a lens it is:

$$\text{FWHM}_{\text{min}}^{\text{lens}} = 0.515 \lambda. \quad (4)$$

The least area of the focal spot determined by the area at half maximum (HMA):

$$\text{HMA}_{\text{min}}^{\text{lens}} = \pi \left(\text{FWHM}_{\text{min}}^{\text{lens}} / 2 \right)^2 \approx 0.21 \lambda^2. \quad (5)$$

The longitudinal size of the focal spot is related with the conception depth of focus (DOF), which in the case of diffraction-limited systems can be evaluated as:

$$\text{DOF}_{\text{lens}} = \frac{\lambda}{2 \sin^2 \theta} \geq 0.5 \lambda. \quad (6)$$

From (6) it follows that with the growing numerical aperture the depth of focus decreases and approaches half the wavelength.

It is also known that when a lens is used with a narrow ring diaphragm [29], the intensity distribution in the focal plane behaves as a zero-order Bessel function $J_0(k\alpha_0\rho)$ whose zero occurs at a less value $J_0(\gamma_{01}) = 0$, $\gamma_{01} = 2.405$. Therefore, the minimal focal spot in this case can have a less radius. However, the efficiency of this approach is very low because the most part of the incident light is absorbed by the stop.

The intensity distribution obeying the zero-order Bessel function $|J_0(k\alpha_0\rho)|^2$ can be also generated with the aid of more effective optical elements: refractive axicon [30], linear diffractive axicon, or binary kinoform lens [31].

The complex transfer function of a diffractive axicon can be written as

$$\tau_{\text{ax}}(r) = \exp(-ik\alpha_0 r), \quad (7)$$

where parameter α_0 determines the convergence angle θ of rays going from the axicon to the optical axis:

$$\alpha_0 = \sin \theta \quad (8)$$

and is, in fact, the numerical aperture of the axicon.

The radius of the central spot in the free space is:

$$\rho_{\text{ax}} = \frac{2.405}{k\alpha_0} = \frac{0.38}{\sin \theta} \lambda \geq 0.38 \lambda. \quad (9)$$

The light spot size at half maximum for the axicon (Fig. 2) is:

$$\text{FWHM}_{\text{min}}^{\text{ax}} = 0.357 \lambda, \quad (10)$$

and the least area of the focal spot is:

$$\text{HMA}_{\min}^{\text{ax}} = \pi \left(\text{FWHM}_{\min}^{\text{ax}} / 2 \right)^2 = 0.1 \lambda^2. \quad (11)$$

The axial extent of the focal spot (the longest distance of diffraction-free propagation of the beam) is:

$$z_{\max}^{\text{ax}} = \frac{R}{\alpha_0}, \quad (12)$$

and with $\sin \theta \rightarrow 1$ the DOF of the axicon is equal to the radius R of the optical element.

All the above-mentioned elements must have the limit numerical aperture to obtain the minimal value (the diffraction limit).

However, if we take a tandem of two optical elements, e.g. lensacon [2], we can generate a nearly-diffraction-limit focal spot with “weaker” optics [1].

If a converging axicon is used, the complex transfer function of the lensacon has the form:

$$\tau_{lx}(r) = \exp \left[-ik \left(\alpha_0 r + \frac{r^2}{2f} \right) \right]. \quad (13)$$

In this case we have a Bessel beam [1]:

$$I_{lx}(\rho, z) \sim \frac{2\pi A^2}{z\alpha_0} \left(\frac{\alpha_0 f z}{f-z} \right)^3 J_0^2 \left(\frac{k\alpha_0 f}{f-z} \rho \right) = \eta(z) J_0^2 [\beta(z)\rho], \quad (14)$$

which decreases in a scalable manner over the range of distances z extending as long as

$$z_{\max}^{lx} = \frac{R}{\alpha_0 + R/f} \leq z_{\max}^{\text{ax}}. \quad (15)$$

The smallest radius of the central spot is at the end of this range of scalable self-reproduction:

$$\rho_{\min}^{lx} = \frac{2.405}{2\pi(\sin \theta + R/f)} \lambda = \frac{0.38}{(\sin \theta + R/f)} \lambda. \quad (16)$$

In the general case, this radius is less than that of the focal spot produced by either element of the tandem.

Depending on the relation between α_0 and the numerical aperture of the lens, adding the axicon to lens (or vice versa, the lens to axicon) can result in a significant reduction of the central spot. In particular, if $\alpha_0 = 0.5$ ($\rho_{\text{ax}} = 0.76\lambda$) and $R/f = 0.5$ ($\rho_{\text{ls}} = 1.22\lambda$), the result is to be the theoretical limit for the axicon: $\rho_{\min}^{lx} = 0.38\lambda$. When $R = 2000\lambda$ (about 1mm for visible-range wavelengths), $z_{\max}^{\text{ax}} = 2R \approx 2$ mm and $z_{\max}^{lx} = R \approx 1$ mm.

The Fresnel transformation for axially symmetric fields can be used in computer simulation of work of the lensacon in the paraxial case:

$$F(\rho, z) = \frac{k}{iz} \exp(ikz) \exp \left(\frac{ik\rho^2}{2z} \right) \int_0^\infty \tau(r) \exp \left(\frac{ikr^2}{2z} \right) J_0 \left(\frac{kr\rho}{z} \right) r dr. \quad (17)$$

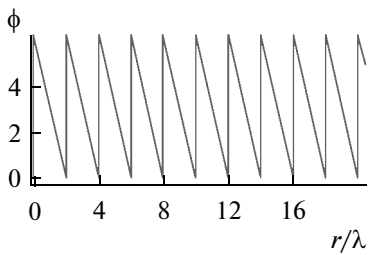

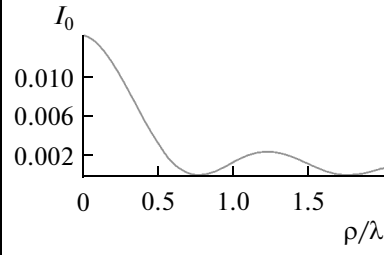
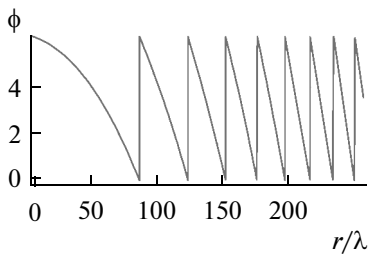

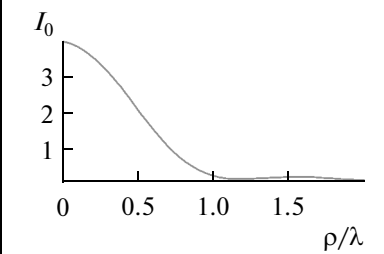
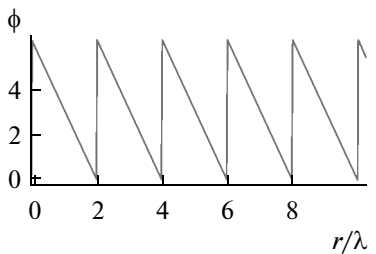
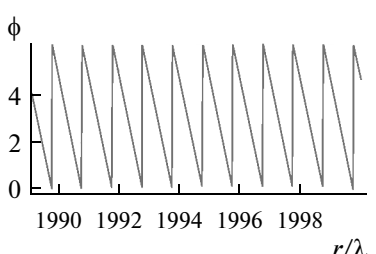
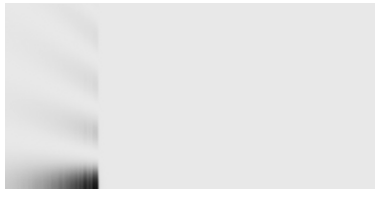
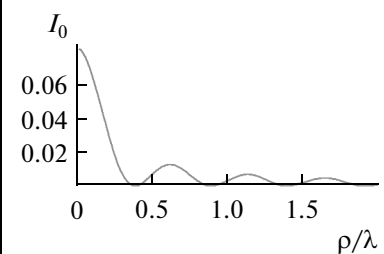
Table 1 gives the computation results for $\lambda = 0.5$ μm , $R = 1$ mm, $f = 2$ mm (numerical aperture $NA = R/f = 0.5$), $\alpha_0 = 0.5$. Twenty samples per a wavelength were used for the both integrands, the axial area 2λ (1 μm) in radius being quantized with 50 samples per a wavelength. The longitudinal intensity distribution was computed for $z \in [0.5 \text{ mm}, 2.5 \text{ mm}]$.

The computer simulation results quite agree with the above-mentioned conclusions. The patterns of axial propagation show clearly how the energy are distributes along the optical axis.

On one hand, adding the lens to axicon results in reducing twofold the self-reproduction interval of the diffraction-free beam of a single axicon; on the other hand, a more compact focal spot is generated with the central-spot intensity being almost an order of magnitude as high.

As compared to a single lens, the intensity of the focal spot of the tandem is nearly five times lower, but at the same time the depth of focus is 40 times longer.

Table 1. Medium-aperture lensacon in the paraxial approach

	Input phase, $z = 0, R = 2000\lambda = 1 \text{ mm}$	Longitudinal intensity picture (a negative), $x \uparrow z$ $z \in [0.5 \text{ mm}, 2.5 \text{ mm}], \rho \in [0, 2\lambda]$	Radial intensity profile in plane Z
Axicon, $\alpha_0 = 0.5$			 $Z = 1.5 \text{ mm}, \rho_0 = 0.77\lambda,$ $\text{max} = 0.014$
Lens, $NA = 0.5$			 $Z = 2 \text{ mm}, \rho_0 = 1.21\lambda, \text{max} = 3.97$
Lensacon	 		 $Z = 0.95 \text{ mm}, \rho_0 = 0.38\lambda,$ $\text{max} = 0.085, \text{FWHM} = 0.36\lambda$

2. A LENSACON WITH A LARGE-APERTURE LENS: THE NON-PARAXIAL VECTOR MODEL IN THE DEBYE APPROACH

Let us consider a large-aperture aplanatic focusing optical system in which the distance between the focal plane and aperture is much greater than a wavelength. Then in a homogeneous dielectric medium the electric vector field near the focus can be expressed in the Debye approach [32, 33]:

$$\mathbf{E}(\rho, \varphi, z) = -\frac{if}{\lambda} \int_0^{\alpha} \int_0^{2\pi} B(\theta, \phi) T(\theta) \mathbf{P}(\theta, \phi) \exp[ik(\rho \sin \theta \cos(\phi - \varphi) + z \cos \theta)] \sin \theta d\theta d\phi, \quad (18)$$

where (θ, ϕ) are spherical coordinates of the output pupil, $B(\theta, \phi)$ is the transfer function, $T(\theta)$ is the pupil apodization function, $\mathbf{P}(\theta, \phi)$ is the polarization matrix which is defined by polarization coefficient of the

incident beam, $n \sin \alpha = NA$, n is the refraction index of the medium, NA is the numerical aperture of the lens, f is the focal length.

If the transfer function is independent of polar angle ϕ ($B(\theta, \phi) = B(\theta)$), relation

$$\int_0^{2\pi} \exp(i\tau \cos(\phi - \varphi)) \exp(im\phi) d\phi = 2\pi i^m J_m(\tau) \exp(im\varphi) \quad (19)$$

can be used to reduce expression (18) to a single integral over azimuth angle:

$$\mathbf{E}(\rho, \varphi, z) = -i^{m+1} k f \exp(im\varphi) \int_0^\alpha B(\theta) T(\theta) \mathbf{Q}(\rho, \varphi, \theta) \exp[ikz \cos \theta] \sin \theta d\theta, \quad (20)$$

where $\mathbf{Q}(\rho, \varphi, \theta)$ depends on the input field polarization [26].

In the aplanatic system the radial component is converted by the sine rule $r = f \sin \theta$ and the pupil apodization function is assumed to be $T(\theta) = \sqrt{\cos \theta}$.

2.1. Linear x -Polarization

Most modern lasers have linear polarization. Matrix $\mathbf{P}(\theta, \phi)$ for linear x -polarization is:

$$\mathbf{P}(\theta, \phi) = \begin{bmatrix} 1 + \cos^2 \phi (\cos \theta - 1) \\ \sin \phi \cos \phi (\cos \theta - 1) \\ -\cos \phi \sin \theta \end{bmatrix}. \quad (21)$$

Let us consider a lens incorporating a large-aperture lens of focus $f = 101\lambda$ and radius $R = 100\lambda$. In the infrared (e.g. $\lambda = 10 \mu\text{m}$) an element like that can't be regarded as micro-optics because $R = 100\lambda = 1 \text{ mm}$ is large enough to conduct experiments.

In the Debye approximation we can guarantee correct results if the Fresnel number

$$N_F = \frac{R^2}{\lambda f} \quad (22)$$

is high. In our case $N_F \approx 100$ is high enough [32].

The x -component makes a major contribution to the axial intensity distribution:

$$E_x(\rho, z) = -\frac{kf}{2} \int_0^\alpha B(\theta) \exp(ikz \cos \theta) \sqrt{\cos \theta} (1 + \cos \theta) J_0(k\rho \sin \theta) \sin \theta d\theta. \quad (23)$$

Adding a narrow ring-shaped stop ($B(\theta) = \delta(\theta - \theta_0)$) to the lens results in formation of a field that is proportional to a zero-order Bessel function and independent of defocusing distance z :

$$|E_x(\rho, z)|^2 = \frac{(kf)^2}{4} J_0^2(k\rho \sin \theta_0) |\cos \theta_0 (1 + \cos \theta_0)^2 \sin^2 \theta_0|. \quad (24)$$

The central spot radius is dependent on azimuth angle θ_0 and can't be less than





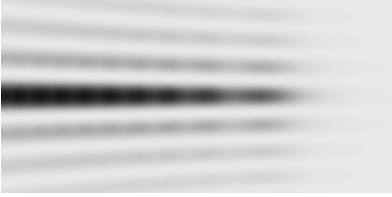

$$\rho_{\min}^\delta = 0.38\lambda. \quad (25)$$

If an axicon is used as $B(\theta)$, the axial distribution (at $\rho = 0$) complies with the expression:

$$E_x(0, z) = \frac{kf}{2} \int_0^\alpha \exp[ik(z \cos \theta - \alpha_0 f \sin \theta)] \sqrt{\cos \theta} (1 + \cos \theta) \sin \theta d\theta. \quad (26)$$

It follows from (26) that with small numerical apertures (i.e. with small θ) the effect of the axicon is small, with the growing numerical aperture the effect becomes more significant, and with $\cos(\theta) \rightarrow 0$ we don't see any z dependence.

Table 2. The focal longitudinal and transverse intensity distributions for linear x -polarization

	Longitudinal intensity picture $x \uparrow z$	Transverse intensity picture $y \uparrow x$
Lens, $f = 101\lambda$	$z \in [81\lambda, 121\lambda], x \in [-2\lambda, 2\lambda]$ 	 $Z = 101\lambda$: FWHM (—) = 0.76λ , FWHM () = 0.48λ
Lensacon, $\alpha_0 = 0.1$	$z \in [61\lambda, 101\lambda], x \in [-2\lambda, 2\lambda]$ 	 $Z = 95\lambda$: FWHM (—) = 0.82λ , FWHM () = 0.36λ
Lensacon, $\alpha_0 = 0.5$	$z \in [61\lambda, 101\lambda], x \in [-2\lambda, 2\lambda]$ 	 $Z = 87\lambda$: FWHM (—) = 0.84λ , FWHM () = 0.32λ

The computation results for a single lens of focus $f = 101\lambda$ and radius $R = 100\lambda$ and the same lens complemented with various axicons are given in Table 2. The number of samples along the azimuth angle is 2001, the transverse size of the calculated area in the focal plane is $4\lambda \times 4\lambda$.

As seen from Table 2, complementing the lens with axicons stretches the focus along the optical axis. The greater the numerical aperture of the axicon, the more the focus elongates in the longitudinal direction and the more it narrows in the transverse direction.

Given sharp focusing, a lensacon with a “weak” axicon generates a beam whose properties are close to those predicted by the paraxial model. However, due to the longitudinal component the focal spot is not symmetric. Note that if we use a powerful lens with even “weak” axicon (say, $\alpha_0 = 0.1$), in vertical direction we can reach the limit that is provided by a single large-aperture axicon: FWHM = 0.36λ (the second row in Table 2).

With a high-NA axicon (e.g. $\alpha_0 = 0.5$), it is possible in vertical direction to overcome the diffraction limit for both the lens and axicon: FWHM = 0.32λ (the third row in Table 2). Further increase of α_0 doesn't cause a significant decrease of the vertical size of the focal spot. At the same time the focus will elongate in the axial direction and the energy in the center of the spot will fall.

Figure 3 shows the longitudinal and transverse focal distributions for a lensacon of radius $R = 100\lambda$ consisting of a lens of focal length $f = 101\lambda$ (NA = 0.95) and an axicon with parameter α_0 changing from 0 (no axicon) to 0.95.

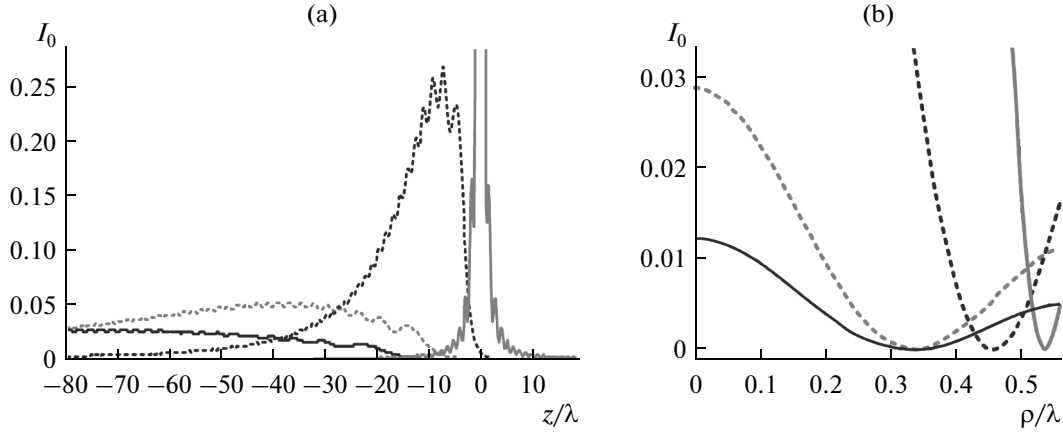


Fig. 3. Axial (a) and transverse (vertical) (b) intensity distributions generated in the focal area by a lensacon consisting of a lens with $\text{NA}=0.95$ ($R=100, f=101\lambda$) and different axicons: with $\alpha_0=0$ (no axicon, grey solid line), $\alpha_0=0.1$ (black dot line), $\alpha_0=0.5$ (grey dot line), and $\alpha_0=0.95$ (black solid line).

In the vector non-paraxial case the transverse intensity profile is not symmetric, so Fig. 3b gives the vertical intensity profile when the total intensity is equal to the intensity of the x -component. As seen from Fig. 3b, the transverse extent of the central spot stops decreasing after the numerical aperture becomes greater than $\alpha_0=0.5$.

2.2. Radial Polarization

Matrix $\mathbf{P}(\theta, \phi)$ for radial polarization is

$$\mathbf{P}(\theta, \phi) = \begin{bmatrix} \cos \phi \cos \theta \\ \sin \phi \cos \theta \\ -\sin \theta \end{bmatrix}. \quad (27)$$

When we use a large-NA focusing optical system for beam with radial polarization, the longitudinal component [26] makes a major contribution to the total axial intensity distribution:

$$E_z(\rho, z) = -kf \int_0^\alpha B(\theta) \exp(ikz \cos \theta) \sqrt{\cos \theta} J_0(k\rho \sin \theta) \sin^2 \theta d\theta. \quad (28)$$

Applying a narrow ring-shaped stop to the lens also results in generation of the field corresponding to the zero-order Bessel function:

$$|E_z(\rho, z)|^2 = (kf)^2 J_0^2(k\rho \sin \theta_0) |\cos \theta_0 \sin^4 \theta_0|. \quad (29)$$

Yet with $\theta_0 \rightarrow 90^\circ$ the intensity (29) will be much higher than in (24). In particular, at $\theta_0 = 82^\circ$ it is three times as high. Nevertheless, diaphragming an optical system brings a decrease in energy efficiency. That is why it is preferable to use phase pupil apodization rather than amplitude apodization. For example, circular binary phase plates are offered in [13, 34] to enhance the contribution of the longitudinal component to the total intensity of the vector field.

If an axicon is used as $B(\theta)$, the axial (with $\rho=0$) intensity profile follows the expression similar to (26):

$$E_z(\rho, z) = -kf \int_0^\alpha \exp[ik(z \cos \theta - \alpha_0 f \sin \theta)] \sqrt{\cos \theta} \sin^2 \theta d\theta. \quad (30)$$

The distance over which the axial intensity keeps almost constant can be determined from the condition:

$$z_{\max} \leq \frac{\varepsilon}{\cos \theta} + \alpha_0 f \tan \theta. \quad (31)$$

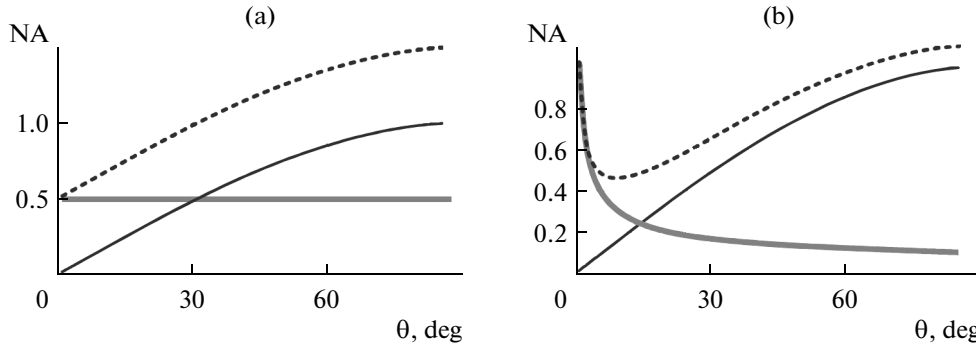


Fig. 4. Numerical aperture (NA) for (a) a lensacon (black solid line corresponds to a large-aperture lens, grey solid line stands for an axicon with $\alpha_0 = 0.5$, dotted line is the total numerical aperture) and (b) a lens complemented with fracxicon $\exp(-i\sqrt{r})$.

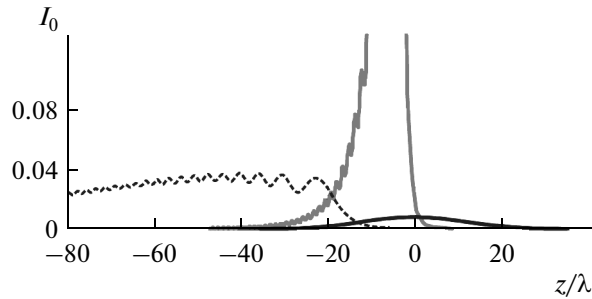


Fig. 5. The axial intensity distribution produced by a lens with a narrow (λ -width slit) annular stop (black solid line), a full-aperture lensacon with $\alpha_0 = 0.1$ (grey solid line), and a lensacon with $\alpha_0 = 0.5$ (dotted line).

It is seen from (31) that if $\theta \rightarrow 90^\circ$ then $z_{\max} \rightarrow \infty$ (similar to the use of a narrow ring-shaped stop). When θ is small, $z_{\max} \leq \varepsilon + \alpha_0 f \theta$, that is, term $\alpha_0 f \theta$ related to the axicon phase function is responsible for the elongation of the interval of small variation of function (30).

So, adding an axicon to a lens increases the numerical aperture of the lens by a constant value, which in the case of large-NA lenses has effect only on rays travelling through the central part (Fig. 4a).

Obviously the best way to compensate the numerical aperture is to supplement a lens with a phase element whose numerical aperture varies as $1 - \sin\theta$. This kind of tandem will work as a “powerful” linear axicon.

An example of complementing a large-aperture lens with a fracxicon [1] of $\exp(-i\alpha\sqrt{r})$ ($\alpha = 1$) is shown in Fig. 4b. In this case the numerical aperture almost never exceeds the limit value for free space and increases considerably in the central part.

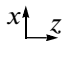


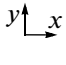
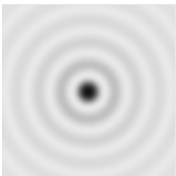
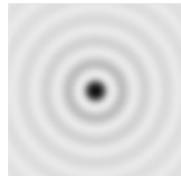
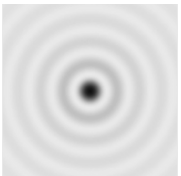
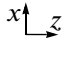

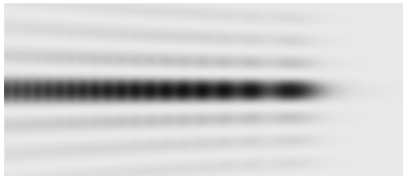
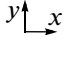
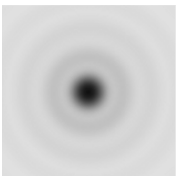
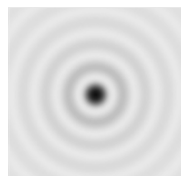
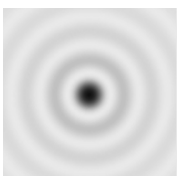
Table 3 gives the computer simulation results of the focusing of a radially-polarized plane wave by a 101λ -focus lens and a lensacon with axicon parameter $\alpha_0 = 0.95$ ($z_{\max}^{\text{ax}} \approx 105\lambda$). In the first case the wave is cut by an annular stop (the radii of the ring are $R_1 = 99\lambda$ and $R_2 = 100\lambda$), in the second case the wave is stopped by a round diaphragm of radius $R = 100\lambda$.

It follows from Table 3 that in the case of radial polarization, the intensity distribution is radially symmetric. The radius of the central light spot corresponds to the minimum of the zero-order Bessel function and won't decrease.

For a lens with a narrow annular stop (slit width is λ) the contribution of transverse components to the focal spot is almost zero. The use of the annular stop results in the energy loss proportional to the area of the blocked central part of the lens.

Free of energy losses, a full-aperture lensacon produces at the focus a cone-shaped intensity distribution. The vertex of the light cone has no transverse component. When we increase the axicon numerical aperture, the focal cone elongates in the axial direction (Table 4) with the intensity distributed almost evenly along the axis (Fig. 5).

Table 3. The longitudinal and transverse focal distributions produced by a lens with a narrow annular stop and by a lensacon with a large-aperture axicon in the case of radial polarization

		$ E ^2$	$ E_z ^2$	
Lens with narrow ring diaphragm	Longitudinal $z \in [61\lambda, 141\lambda]$ 			
	Transverse, $4\lambda \times 4\lambda$ 	 $z = 61\lambda$ FWHM = 0.36λ	 $z = f = 101\lambda$ FWHM = 0.36λ	 $z = 61\lambda$
Lensacon $\alpha_0 = 0.95$	Longitudinal $z \in [21\lambda, 101\lambda]$ 			
	Transverse, $4\lambda \times 4\lambda$ 	 $z = 20\lambda$ FWHM = 0.6λ	 $z = 78\lambda$ FWHM = 0.36λ	 $z = 20\lambda$

Note that the body and vertex of the focal cone consist of only longitudinal component, while “side-lobes” include the transverse components (Fig. 6).

3. VORTICAL LENSACON IN THE DEBYE APPROXIMATION

Paper [26] showed that it is possible to reach sub-wavelength localization of light in sharp focusing of a vortex field. The central light spot is symmetrical for both azimuthal and circular polarization in this case.

With azimuthal polarization the effect of sub-wavelength localization is possible only for the transverse components of the vector electric field. For circular polarization the effect exists for the longitudinal component.

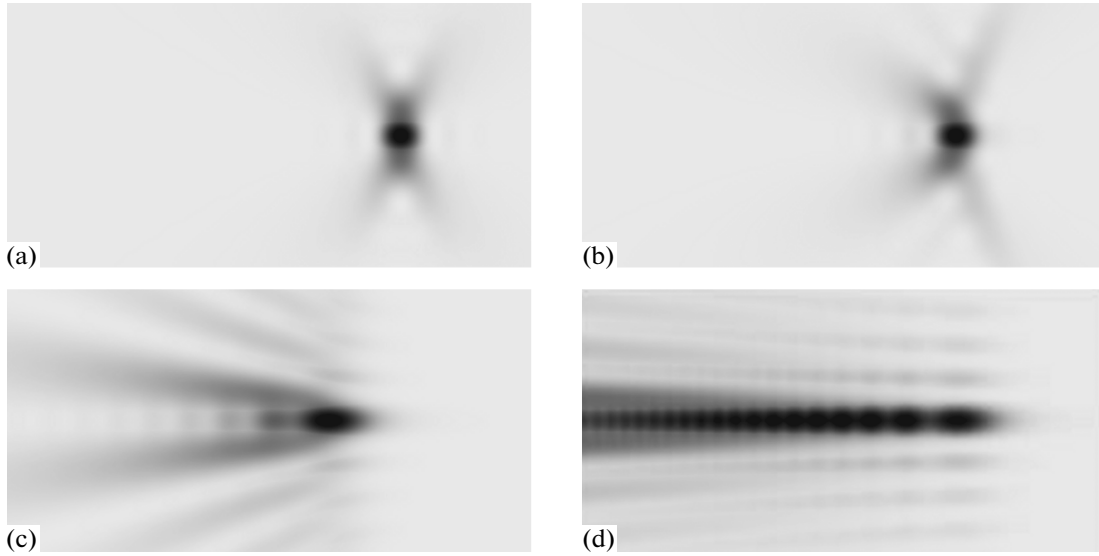


Fig. 6. The longitudinal distribution for a single lens (a) and lensacons with $\alpha_0 = 0.1$ (b), $\alpha_0 = 0.5$ (c) and $\alpha_0 = 0.95$ (d).

3.1. Azimuthal Polarization

For azimuthal polarization described by matrix

$$\mathbf{P}(\theta, \phi) = \begin{bmatrix} \sin \phi \\ -\cos \phi \\ 0 \end{bmatrix} \quad (32)$$

the presence of the vortex phase in the transfer function:

$$B(\theta, \phi) = R(\theta) \exp(im\phi) \quad (33)$$

leads to the following form of the field in the focal area [26]:

$$\mathbf{E}_m(\rho, \varphi, z) = -i^{m+1} k f \exp(im\varphi) \int_0^\alpha \mathbf{Q}_m(\rho, \varphi, \theta) R(\theta) T(\theta) \sin \theta \exp(ikz \cos \theta) d\theta, \quad (34)$$

$$\mathbf{Q}_m(\rho, \varphi, \theta) = \begin{bmatrix} S_m(t) \\ -C_m(t) \\ 0 \end{bmatrix}, \quad (35)$$

where $S_m(t) = \frac{1}{2} [e^{i\varphi} J_{m+1}(t) + e^{-i\varphi} J_{m-1}(t)]$, $C_m(t) = \frac{i}{2} [e^{i\varphi} J_{m+1}(t) - e^{-i\varphi} J_{m-1}(t)]$, $t = k\rho \sin \theta$.

It follows from (32) that the longitudinal component is always missing.

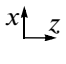


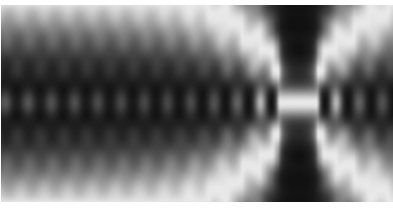

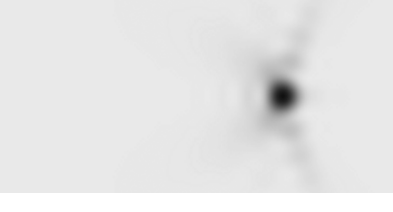


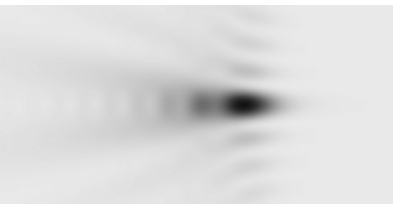
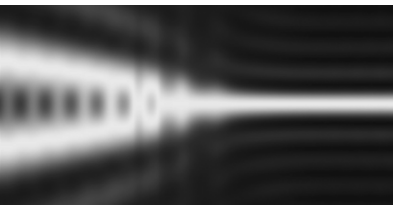
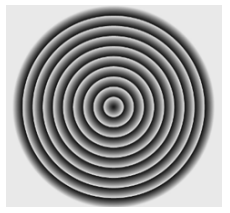
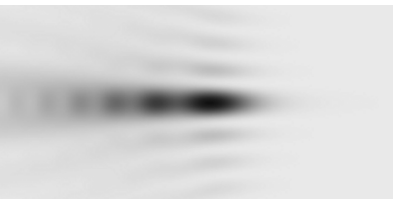
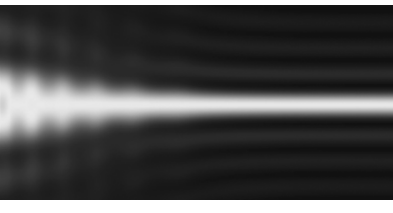
On the optical axis (with $\rho = 0$) field (34) has non-zero components only for one order of vortex phase singularity $|m| = 1$. This allows the components proportional to $J_0(t)$ to appear in (35) (Table 5).

3.2. Circular Polarization

For circular polarization described by matrix

$$\mathbf{P}(\theta, \phi) = \frac{1}{\sqrt{2}} \begin{bmatrix} [1 + \cos^2 \phi (\cos \theta - 1)] \pm i [\sin \phi \cos \phi (\cos \theta - 1)] \\ [\sin \phi \cos \phi (\cos \theta - 1)] \pm i [1 + \sin^2 \phi (\cos \theta - 1)] \\ -\sin \theta [\cos \phi \pm i \sin \phi] \end{bmatrix} \quad (36)$$

Table 4. The longitudinal intensity distribution produced by a full-aperture lens and a lensacon incorporating a small-aperture axicon for radial polarization of the incident light

	Transmission function	Intensity (negative)	Topology
		$z \in [86\lambda, 106\lambda], x \in [-2\lambda, 2\lambda]$ 	
Lens			
Lensacon, $\alpha_0 = 0.01$			
Lensacon, $\alpha_0 = 0.05$			
Lensacon, $\alpha_0 = 0.1$			

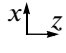
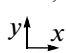
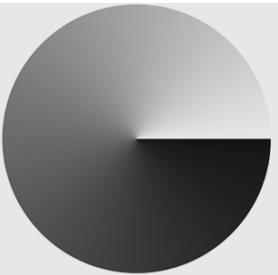
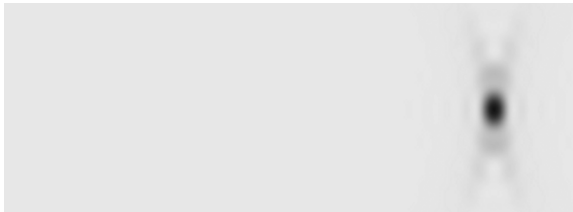

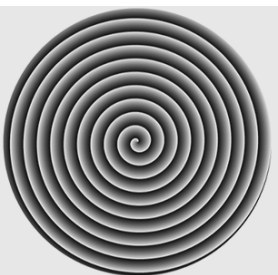
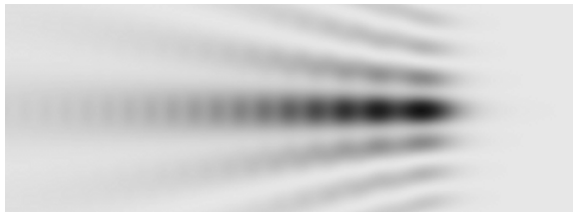

the presence of vortex phase (33) in the transfer function allows the formation of a field of type (34) with vortical matrix [26]:

$$\mathbf{Q}_m(\rho, \varphi, \theta) = \frac{1}{\sqrt{2}} \begin{bmatrix} J_m(t) + \frac{1}{2}[J_m(t) + E2_m(t)](\cos\theta - 1) \\ \operatorname{sgn}(p)i \left\{ J_m(t) + \frac{1}{2}(J_m(t) - E2_m(t))(\cos\theta - 1) \right\} \\ -E1_m(t)\sin\theta \end{bmatrix}, \quad (37)$$

where $E1_m(t) = \operatorname{sgn}(p)e^{i\operatorname{sgn}(p)\varphi} J_{m+\operatorname{sgn}(p)}(t)$, $E2_m(t) = -e^{i\operatorname{sgn}(p)2\varphi} J_{m+\operatorname{sgn}(p)2}(t)$, $t = k\rho \sin\theta$, $\operatorname{sgn}(p)$ is the sign of the input polarization.

On the optical axis (with $\rho = 0$) field (36) will have non-zero components only for vortex phase orders $|m| \leq 2$. This allows the components proportional to $J_0(t)$ to appear in (37) (Tables 6, 7).

Table 5. The longitudinal and transverse distributions of the total intensity for azimuthally polarized beam with vortex phase function ($|m| = 1$) and for a vortical lensacon

	Transmission function	Longitudinal distribution $z \in [-30\lambda, 5\lambda], x \in [-2\lambda, 2\lambda]$ 	Transverse distribution, $4\lambda \times 4\lambda$ 
Lens with vortex incident beam			 $z = f = 101\lambda$ FWHM: 0.5λ
Vortical lensacon, $\alpha_0 = 0.1$			 $z = 96\lambda$ FWHM: 0.41λ

Use of a large-aperture axicon allows a stable extended pattern with a sub-wavelength size of the central spot to form in some components of the vector electric field. This fact should be taken into account when we deal with the interaction of laser radiation with materials that have different sensitivity to different vector components [27].

Use of vortex phase filters makes it possible to select different components (longitudinal or transverse) of the vector field in the axial distribution: the vortex phase singularity compensates polarization singularities [25, 26] and non-zero axial items corresponding to $J_0(t)$ appear in different components, which defines the minimal achievable size of the central spot of the zero-order Bessel beam [9] (i.e. FWHM = 0.36λ).

If we use “weak” vortical axicons (as shown in Table 7), the intensity varies significantly over the interval of scalable self-reproduction, and the compact light spot forms only at the end of the interval. However, the intensity at the vertex of the focal cone can be much higher (see Fig. 5) in this case, which can be important in some applications.

So, the computer simulation results obtained in the Debye approximation show that the use of the tandem consisting of a large-aperture lens and small-aperture axicon allows us to produce a compact light spot. An increase of the axicon numerical aperture causes the transversely compact focal area to stretch in the axial direction with an almost even intensity distribution over this area and lower intensity at each particular axial point.

Table 6. The longitudinal and transverse distributions of the total and component's intensity of the field for a vortical lensacon with $\alpha_0 = 0.95$ ($|m| \leq 2$) and large-aperture lens (NA = 0.95) in the case of circular polarization

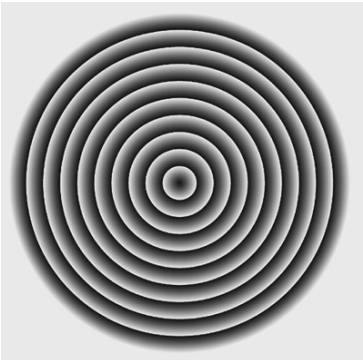

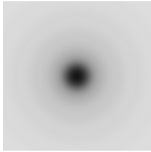
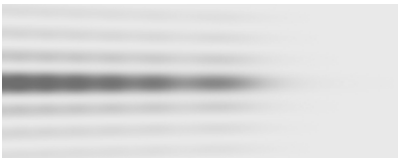
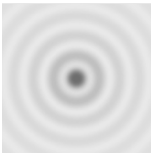
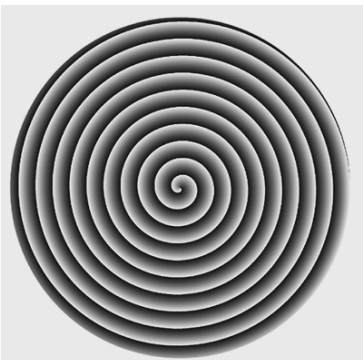
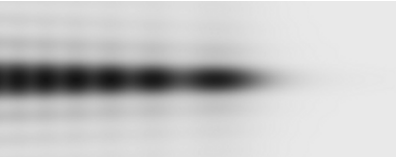
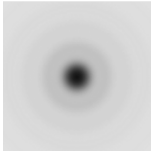
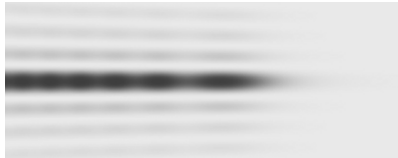
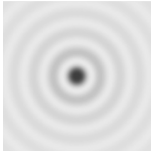
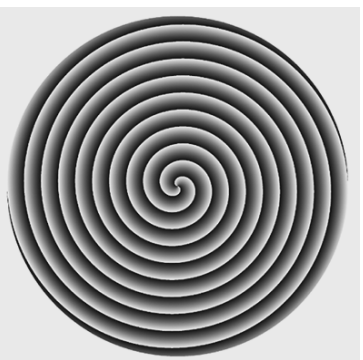
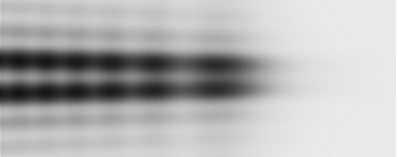
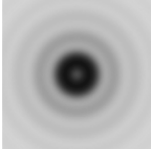
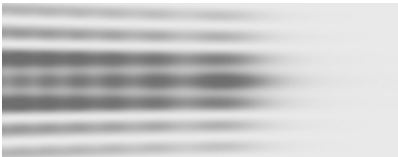
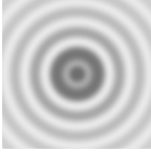
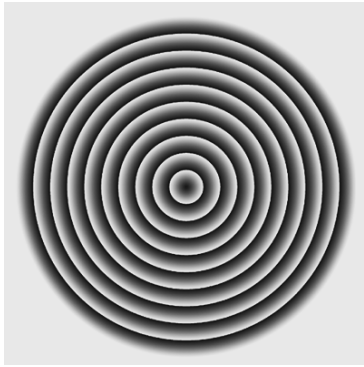

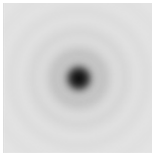

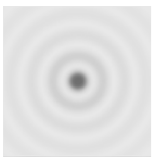
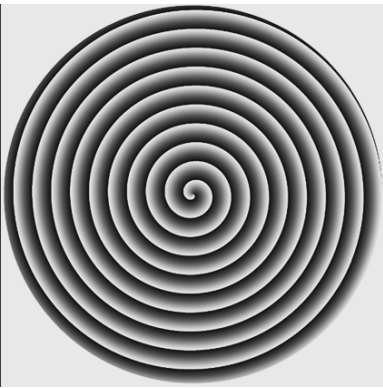



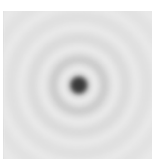
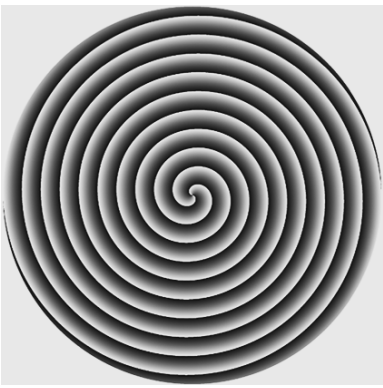
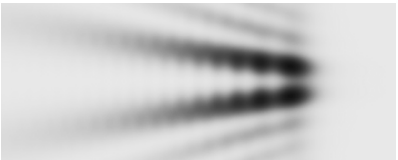
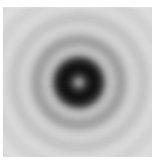

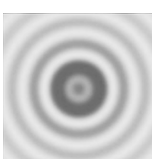
	Central part of input phase	Longitudinal distribution $z \in [-50\lambda, 0\lambda], x \in [-2\lambda, 2\lambda]$ $x \uparrow z \rightarrow$	Transverse distribution, $4\lambda \times 4\lambda z = 96\lambda, y \uparrow x \rightarrow$
$m = 0$		$ E ^2$ 	 FWHM: 0.65λ
		$ E_t ^2$ 	 FWHM: 0.36λ
$m = -1$		$ E ^2$ 	 FWHM: 0.59λ
		$ E_z ^2$ 	 FWHM: 0.36λ
$m = -2$		$ E ^2$ 	 FWHM: 1.17λ
		$ E_t ^2$ 	 FWHM: 0.41λ

Table 7. The longitudinal and transverse distributions of the total and component's intensity of the field for a vortical lensacon with $\alpha_0 = 0.1$ ($|m| \leq 2$) and large-aperture lens (NA = 0.95) in the case of circular polarization

	Central part of input phase	Longitudinal distribution $z \in [-30\lambda, 5\lambda], x \in [-2\lambda, 2\lambda]$ $x \uparrow z \leftarrow$	Transverse distribution, $4\lambda \times 4\lambda, z = 96\lambda$ $y \uparrow x \leftarrow$
$m = 0$		$ E ^2$ 	 FWHM: 0.55λ
		$ E_r ^2$ 	 FWHM: 0.4λ
$m = -1$		$ E ^2$ 	 FWHM: 0.74λ
		$ E_z ^2$ 	 FWHM: 0.4λ
$m = -2$		$ E ^2$ 	
		$ E_r ^2$ 	

CONCLUSIONS

We have considered the use of axicons in large-aperture focusing systems with different polarization in terms of the Debye model.

The investigations confirm that it is possible to decrease the focal spot size generated by a large-aperture lens by complementing the lens with a diffractive axicon (the effect can be observed even with a small-aperture axicon). Being an alternative to the use of annular diaphragms, the approach is more energy effective.

When a lensacon (tandem of lens and axicon) is used, the focal area looks like a cone, which agrees with the results of paraxial modeling [1]. However, unlike the paraxial approach, the integral expressions for the complex amplitude in the focal area allows the size of the central spot of the zero-order Bessel beam to be determined as the smallest achievable size of the focal spot ($\text{FWHM} = 0.36\lambda$). Depending on the “strength” of the diffractive axicon, the sub-wavelength focal spot is spread in the axial direction over some distance.

Nevertheless, in the case of linear polarization the limit can be overcome in one direction ($\text{FWHM} = 0.32\lambda$).

For circular polarization, it is possible to get a decreased size of the axially symmetric focal spot by using vortical axicons. In this case the polarization singularity inherent to circular polarization is compensated [25, 26]. For azimuthal polarization, the compensation is made in a similar way except that the light spot will have a smaller size due to the missing longitudinal component.

We have also demonstrated that the presence of the vortex phase (of the first and second order) in the axicon allows us to control the contribution of different components of the electric field in the core and vertex of the focal cone. Accordingly, it is possible to reach a noticeable sub-wavelength focusing of light for each particular component ($\text{FWHM} = 0.41\lambda$), which may be useful in controlling the interaction of electromagnetic radiation with the materials that react differently to different field components.

However, the model doesn't permit us to get correct results with medium-aperture lenses because the Debye approximation works well only in the case of large Fresnel numbers. The results also become less reliable as we move away from the focal plane, and the use of an axicon results in not only elongation of the focal area, but also its considerable shift towards the optical element.

Accordingly, it is necessary to additionally research the complex amplitudes in the vicinity of the focusing element plane. Rayleigh-Sommerfeld diffraction integrals or the plane-wave expansion approach can be used to solve the problem.

ACKNOWLEDGMENTS

The research was supported by the Russian Foundation for Basic Research (RFBR grants 13-07-00266 and 13-07-97004).

REFERENCES

1. Khonina, S.N., Ustinov, A.V., and Volotovskiy, S.G., Fractional axicon as a new type of diffractive optical element with conical focal region, *Precision Instrum. Mechanol.*, 2013, vol. 2, no. 4, pp. 132–143.
2. Koronkevich, V.P., Mikhaltsova, I.A., Churin, E.G., and Yurlov, Yu.I., Lensacon, *Appl. Opt.*, 1993, vol. 34, no. 25, pp. 5761–5772.
3. Quabis, S., Dorn, R., Eberler, M., Glockl, O., and Leuchs, G., Focusing light to a tighter spot, *Opt. Commun.*, 2000, vol. 179, pp. 1–7.
4. Youngworth, K.S. and Brown, T.G., Focusing of high numerical aperture cylindrical-vector beams, *Opt. Express.*, 2000, vol. 7, pp. 77–87.
5. Dorn, R., Quabis, S., and Leuchs, G., Sharper focus for a radially polarized light beam, *Phys. Rev. Lett.*, 2003, vol. 91, p. 233901.
6. Kozawa, Y. and Sato, S., Sharper focal spot formed by higher-order radially polarized laser beams, *J. Opt. Soc. Am., Ser. A*, 2007, vol. 24, p. 1793.
7. Rao, L., Pu, J., Chen, Z., and Yei, P., Focus shaping of cylindrically polarized vortex beams by a high numerical-aperture lens, *Opt. Laser Technol.*, 2009, vol. 41, pp. 241–246.
8. Kotlyar, V.V. and Stafeev, S.S., Modeling the sharp focus of a radially polarized laser mode using a conical and a binary microaxicon, *JOSA, Ser. B*, 2010, vol. 27, no. 10, pp. 1991–1997.
9. Kalosha, V.P. and Golub, I., Toward the subdiffraction focusing limit of optical superresolution, *Opt. Lett.*, 2007, vol. 32, pp. 3540–3542.

10. Davidson, N. and Bokor, N., High-numerical-aperture focusing of radially polarized doughnut beams with a parabolic mirror and a flat diffractive lens, *Opt. Lett.*, 2004, vol. 29, pp. 1318–1320.
11. Stadler, J., Stanciu, C., Stupperich, C., and Meixner, A.J., Tighter focusing with a parabolic mirror, *Opt. Lett.*, 2008, vol. 33, no. 7, pp. 681–683.
12. Zhan, Q., Cylindrical vector beams: from mathematical concepts to applications, *Adv. Opt. Photon.*, 2009, vol. 1, pp. 1–57.
13. Wang, H., Shi, L., Lukyanchuk, B., Sheppard, C., and Chong, C.T., Creation of a needle of longitudinally polarized light in vacuum using binary optics, *Nature Photon.*, 2008, vol. 2, pp. 501–505.
14. Sick, B., Hecht, B., and Novotny, L., Orientational imaging of single molecules by annular illumination, *Phys. Rev. Lett.*, 2000, vol. 85, pp. 4482–4485.
15. Novotny, L., Beversluis, M.R., Youngworth, K.S., and Brown, T.G., Longitudinal field modes probed by single molecules, *Phys. Rev. Lett.*, 2001, vol. 86, pp. 5251–5254.
16. Zhan, Q. and Leger, J.R., Focus shaping using cylindrical vector beams, *Opt. Express.*, 2002, vol. 10, no. 7, pp. 324–331.
17. Kawauchi, H., Yonezawa, K., Kozawa, Y., and Sato, S., Calculation of optical trapping forces on a dielectric sphere in the ray optics regime produced by a radially polarized laser beam, *Opt. Lett.*, 2007, vol. 32, p. 1839.
18. Romea, R.D. and Kimura, W.D., Modeling of inverse Cherenkov laser acceleration with axicon laser beam focusing, *Phys. Rev., Ser. D*, 1990, vol. 42, no. 5, p. 1807.
19. Gupta, D.N., Kant, N., Kim, D.E., and Suk, H., Electron acceleration to GeV energy by a radially polarized laser, *Phys. Lett., Ser. A*, 2007, vol. 368, pp. 402–407.
20. Beversluis, M.R., Novotny, L., and Stranick, S.J., Programmable vector point-spread function engineering, *Opt. Express.*, 2006, vol. 14, pp. 2650–2656.
21. Yirmiyahu, Y., Niv, A., Biener, G., Kleiner, V., and Hasman, E., Excitation of a single hollow waveguide mode using inhomogeneous anisotropic subwavelength structures, *Opt. Express.*, 2007, vol. 15, no. 20, pp. 13404–13414.
22. Xie, X.S. and Dunn, R.C., Probing single molecule dynamics, *Science*, 1994, vol. 265, pp. 361–364.
23. Khonina, S.N., Kotlyar, V.V., Soifer, V.A., Shinkaryev, M.V., and Uspleniev, G.V., Trochoson, *Opt. Commun.*, 1992, vol. 91, no. 3-4, pp. 158–162.
24. Khonina, S.N., Kotlyar, V.V., Skidanov, R.V., Soifer, V.A., Jefimovs, K., Simonen, J., and Turunen, J., Rotation of microparticles with Bessel beams generated by diffractive elements, *J. Mod. Opt.*, 2004, vol. 51, no. 14, pp. 2167–2184.
25. Zhan, Q., Properties of circularly polarized vortex beams, *Opt. Lett.*, 2006, vol. 31, no. 7, pp. 867–869.
26. Khonina, S.N., Kazanskiy, N.L., and Volotovskiy, S.G., Influence of vortex transmission phase function on intensity distribution in the focal area of high-aperture focusing system, *Opt. Mem. Neural Networks (Inform. Opt.)*, 2011, vol. 20, no. 1, pp. 23–42.
27. Grosjean, T. and Courjon, D., Photopolymers as vectorial sensors of the electric field, *Opt. Express.*, 2006, vol. 14, no. 6, pp. 2203–2210.
28. Goodman, J.W., *Introduction to Fourier Optics*, New York: McGraw-Hill Book Company, Inc., 1968, p. 441.
29. Durnin, J., Exact solutions for nondiffracting beams, I: The scalar theory, *J. Opt. Soc. Am., Ser. A*, 1987, vol. 4, no. 4, pp. 651–654.
30. McLeod, J.H., The axicon: a new type of optical element, *J. Opt. Soc. Am.*, 1954, vol. 44, pp. 592–597.
31. Fedotovskiy, A. and Lehovc, H., Optical filter design for annular imaging, *Appl. Opt.*, 1974, vol. 13, no. 12, pp. 2919–2923.
32. Richards, B. and Wolf, E., Electromagnetic diffraction in optical systems, II: Structure of the image field in an aplanatic system, *Proc. Royal Soc., Ser. A*, 1959, vol. 253, pp. 358–379.
33. Helseth, L.E., Optical vortices in focal regions, *Opt. Commun.*, 2004, vol. 229, pp. 85–91.
34. Wang, H. and Gan, F., High focal depth with a pure-phase apodizer, *Appl. Opt.*, 2001, vol. 40, no. 31, pp. 5658–5662.